Biophysical Characterization of Genetically Encoded Voltage Sensor ASAP1: Dynamic Range Improvement

Elizabeth E. L. Lee[1] and Francisco Bezanilla[1,2,*]

[1]Committee on Neurobiology and [2]Department of Biochemistry and Molecular Biology and Institute for Biophysical Dynamics, University of Chicago, Chicago, Illinois

ABSTRACT   Recent work has introduced a new fluorescent voltage sensor, ASAP1, which can monitor rapid trains of action potentials in cultured neurons. This indicator is based on the *Gallus gallus* voltage-sensitive phosphatase with the phosphatase domain removed and a circularly permuted GFP placed in the S3-S4 linker. However, many of the biophysical details of this indicator remain unknown. In this work, we study the biophysical properties of ASAP1. Using the cut-open voltage clamp technique, we have simultaneously recorded fluorescence signals and gating currents from *Xenopus laevis* oocytes expressing ASAP1. Gating charge movement and fluorescence kinetics track closely with each other, although ASAP1 gating currents are significantly faster than those of *Ciona intestinalis* voltage-sensitive phosphatase. Altering the residue before the first gating charge removes a split in the ASAP1 QV curve, but preserves the accelerated kinetics that allow for the faithful tracking of action potentials in neurons.

The hunt for a robust, genetically encoded voltage indicator (GEVI) has been ongoing for the last several decades (1). Although some rely on rhodopsin constructs (2), alternative GEVI designs capitalize on modifications of stereotypical S4-type voltage sensors like ArcLight and VSFP2.3 (3,4). Accelerated sensor of action potentials 1 (ASAP1) (5), is based on a mutated voltage-sensing domain of *Gallus gallus* (GgVSD) voltage-sensitive phosphatase, where a circularly permuted GFP (cpGFP) (6) is added in the S3-S4 linker, making the fluorophore extracellular. The first arginine of GgVSD is mutated to a glutamine (R153Q), shifting the voltage dependence. Previous studies have demonstrated the ability of ASAP1 and its subsequent versions to follow action potentials in neurons in vitro (5) and in vivo (7). Yet, a deeper understanding of the mechanism of ASAP1 could generate a more versatile GEVI. By incorporating rationally chosen mutations, we can evaluate the degree to which this voltage-sensitive phosphatase resembles, functionally and structurally, the extensively investigated *Ciona intestinalis* voltage sensitive phosphatase (CiVSP). This

way we can determine the nature of its accelerated kinetics, and engineer faster and more robust voltage indicators. We expressed ASAP1 in *Xenopus laevis* oocytes and simultaneously recorded gating currents (Fig. 1 *A*) and fluorescence signals (Fig. 1 *B*) using the cut-open voltage clamp method (8). ASAP1 displays a striking split in both electrophysiological and optical signals, indicating the presence of an intermediate state (Fig. 1 *C*). The fluorescence signal shows high fidelity to the movement of the gating charge. Both the kinetics of fluorescence and gating charge movement have a slow and a fast component, where the majority of the kinetics is determined by the fast component (Table S1). The fast component of the gating charge time constants (τ_{fast}) and the fluorescence signal are in the 1–4 ms range (Fig. 1 *D*). Another important metric for all GEVIs is the time it takes for the fluorescence to change in response to a change in voltage, called the fluorescence lag. For ASAP1, this lag is in the submillisecond range and represents a large improvement compared with other GEVIs (Fig. 2).

The split in the QV creates a plateau between −100 and 0 mV, which occurs in both the QV and FV and points to a stable intermediate state. This clearly limits the dynamic potential of ASAP1 and subsequent versions like ASAP2f by limiting the fluorescence read-out in the physiological voltage range (Fig. S1). A large split in the QV is not a property shared by other voltage-sensitive
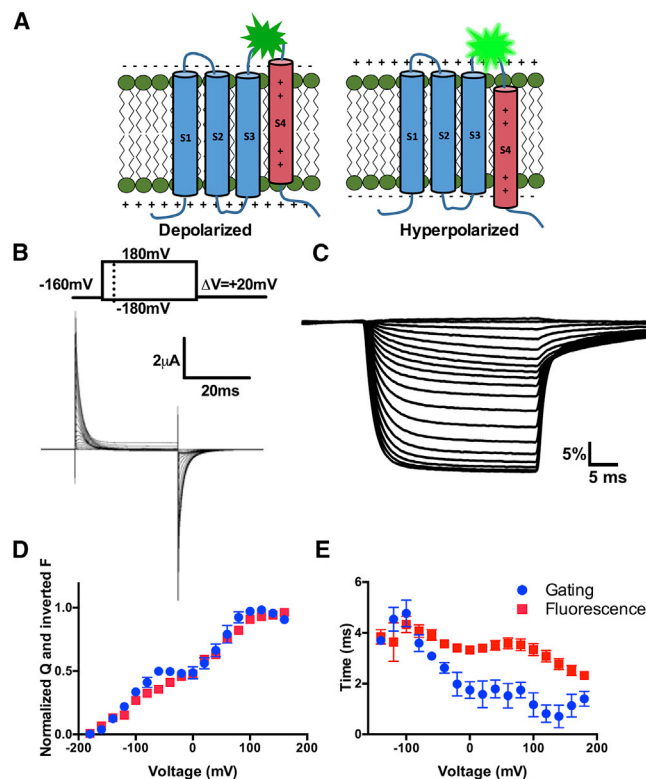
CrossMark

FIGURE 1 Biophysical characterization of ASAP1. (*A*) A cartoon representation of the design of ASAP1. (*B*) Representative gating current recordings of ASAP1. The inset describes the pulse protocol. From a holding potential of −60 mV, a 50 ms prepulse to −160 mV is followed by a 30 ms variable voltage pulse from −180 to 180 mV in increments of 20 mV, with a 50 ms postpulse at −160 mV. (*C*) Representative traces of ASAP1 fluorescence, with the same pulse procedure. (*D*) Normalized QV and 1-FV$_{normalized}$ (inverted fluorescence) curves for ASAP1. (*E*) A comparison of the activation τ_{fast} of the gating charge and the fluorescence of ASAP1. Gating as circles and fluorescence as squares; $n = 11$. To see this figure in color, go online.

phosphatases (9), thus we hypothesized that this phenomenon might be related to the addition of the GFP in the S3-S4 linker. Indeed, removal of the cpGFP from ASAP1, also known as GgVSD R153Q, leads to a sensor with a
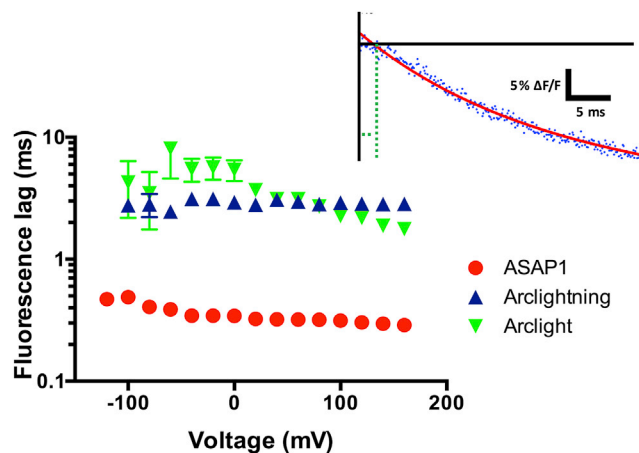
FIGURE 2 Small fluorescence lag in ASAP1. A comparison of fluorescence lags, calculated from double exponential fits (see *inset*), of different GEVIs as a function voltage with ASAP1 as circles, ArcLight as inverted triangles, and ArcLightning in triangles shows a very short lag for ASAP1. Inset: Data are the small dots, the fitted curve is the solid line, and the fluorescence lag is measured as the distance from the intersection of the fitted curve to the *x* axis, as shown with the dashed line. ASAP1: $n = 11$; ArcLight: $n = 5$; ArcLightning: $n = 5$. To see this figure in color, go online.

QV curve fitted by a two-state model (a single Boltzmann). Fig. 3 shows that the kinetics and steady-state features of GgVSD and ASAP1 are drastically different from one another as a result of the addition of a cpGFP to the S3-S4 linker. We reasoned that addition of the cpGFP led to an acceleration in gating current kinetics not seen in other voltage-sensitive phosphatases (9,10).

Residues in the hydrophobic plug of ASAP1 are similar to those in CiVSP, such as I126 (11). Moreover, gating and fluorescence kinetics in ASAP1 are very similar to each other. Therefore, we hypothesized that alterations of these similar hydrophobic plug residues in ASAP1 would result in accelerated gating. However, although some of the mutations effectively altered the biophysical properties of ASAP1 (Fig. S2), the analogous mutations in CiVSP did not improve the fluorescence signal or accelerate sensing kinetics. This may be due to the cpGFP in the linker.
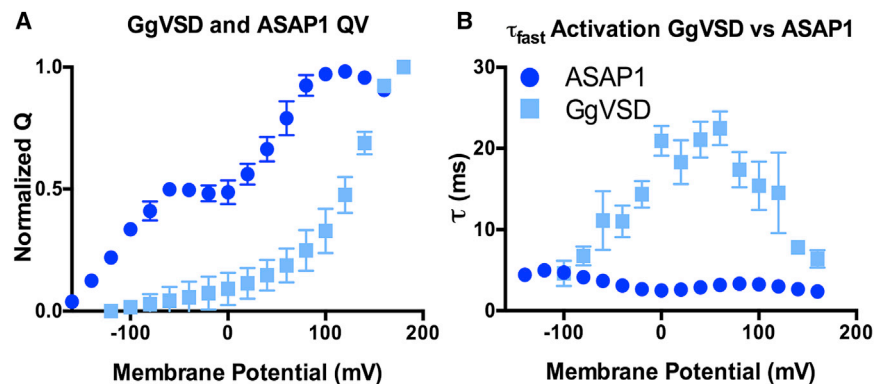

FIGURE 3 Biophysical characterization of GgVSD. (*A*) A comparison of the QV curves of GgVSD (*square*) versus ASAP1 (*circle*). (*B*) A comparison of the fast activation τ of GgVSD and ASAP1. Error bars are within the symbols. ASAP1: $n = 11$; GgVSD: $n = 6$. To see this figure in color, go online.
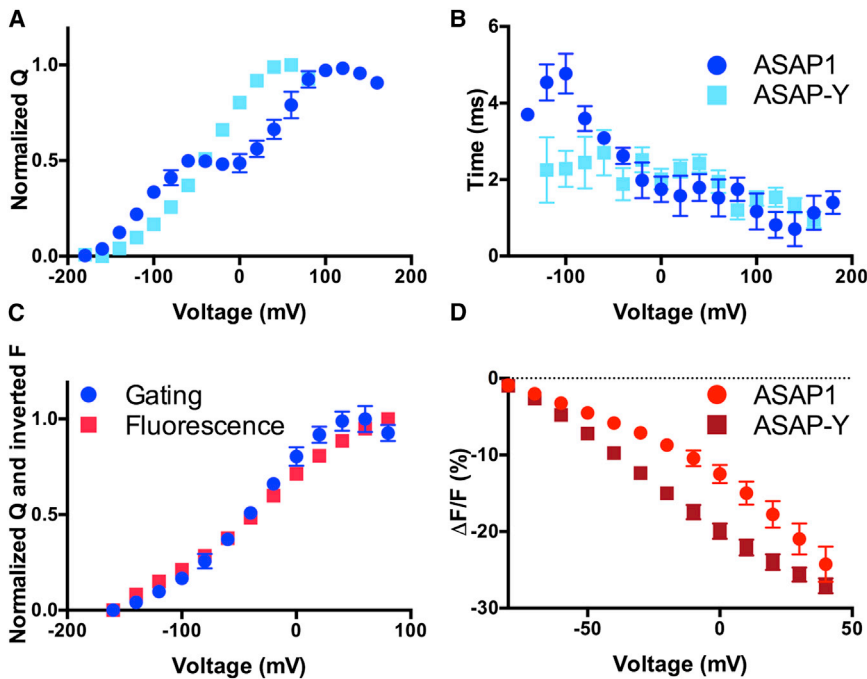
FIGURE 4 Biophysical characterization of ASAP-Y and comparison to ASAP1. (*A*) Normalized QV curves for ASAP1 (*circle*) and ASAP-Y (*square*). (*B*) A comparison of the activation τ_{fast} of the gating charge for ASAP1 and ASAP-Y. (*C*) Normalized QV (*circle*) and 1-FV$_{normalized}$ (*square*) curves for ASAP-Y. (*D*) A comparison of the $\Delta F/F$ % in a physiological range of ASAP1 (*circle*) and ASAP-Y (*square*). (ASAP1: $n = 8$; ASAP-Y: $n = 6$). To see this figure in color, go online.

Recent work (12) in the voltage-gated potassium channel Shaker has demonstrated the importance of nonsensing residues in position 361 for tuning the voltage dependence of the voltage-sensing domain, and we have used this knowledge to further improve on ASAP1. Changing leucine 158 to a tyrosine removed the intermediate state in the QV curve, but preserved the accelerated kinetics and large signal (Fig. 4, A–C). The τ_{fast} of the gating charge and the fluorescence were 1.95 ± 0.29 and 1.74 ± 0.23 ms (mean ± SE) at 60 mV, respectively. Change of this magnitude in the QV and FV curves within the physiological range generates a larger dynamic range than ASAP1 (Fig. 4 D). We named this new variant of ASAP1, ASAP-Y.
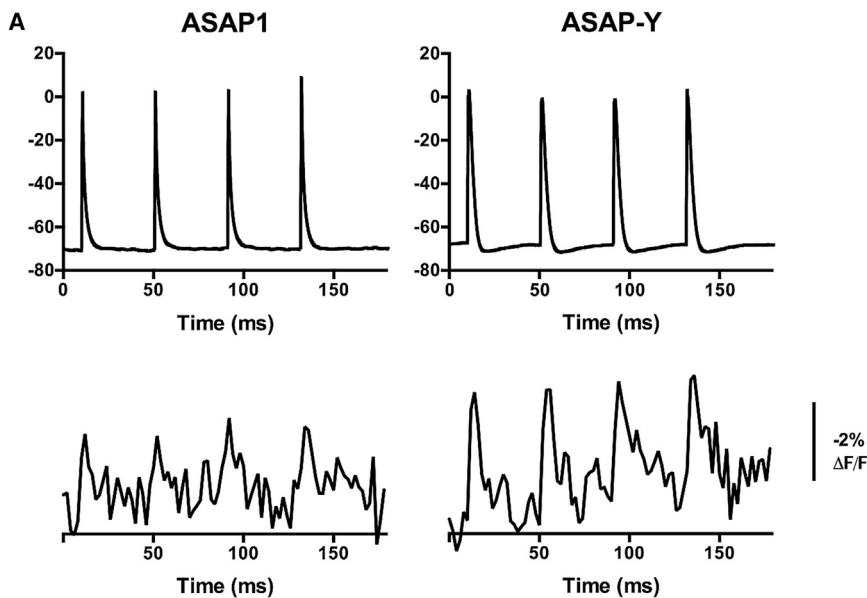

FIGURE 5 ASAP-Y can follow action potentials in rat dorsal root ganglion neurons. (*A*) Representative traces of action potentials from dorsal root ganglion neurons transfected with ASAP1 (*left*) and ASAP-Y (*right*). Corresponding fluorescence traces are shown below as $-\Delta F/F$ (%). (*B*) A table comparing the $-\Delta F/F$ per 100 mV and deactivation τ of ASAP1 and ASAP-Y fluorescence. ASAP1: $n = 11$; ASAP-Y: $n = 13$.

B

	ASAP1	ASAP-Y
ΔF/F per 100 mV (%)	-7.45±0.80	-9.49±0.77
Deactivation τ (ms)	6.52±0.51	4.63±0.44

To determine the effectiveness of our new tool, we transfected rat dorsal root ganglion neurons with ASAP1 and ASAP-Y and recorded action potentials using whole-cell patch clamp. ASAP-Y has comparable transfection efficiency and photobleaching properties to ASAP1 (Fig. S3). We observed fluorescence read-outs of action potentials with both ASAP1 and ASAP-Y and demonstrated increased signal amplitude with ASAP-Y, even though the voltage range spanned by the action potentials in both cases was similar (Fig. 5 *A*). This result is expected when comparing the FV curves of ASAP1 and ASAP-Y (Figs. 1 *D* and 4 *C*). Furthermore, ASAP-Y displayed faster kinetics on the return to baseline than ASAP1 (Fig. 5 *B*).

We found that the fast kinetics of ASAP1 and ASAP-Y are due to the addition of the cpGFP in the S3-S4 loop. This observation is in line with the reported crystal structures of CiVSP in the resting and activated states (13), where it was found that the position of this loop changes drastically during activation.

In conclusion, a rational design method has allowed us to improve upon an existing GEVI to create ASAP-Y. This is, to our knowledge, a novel optical voltage probe with a steeper fluorescence response in the physiological range of voltage changes.

SUPPORTING MATERIAL

Supplemental Materials and Methods, three figures, and one table are available at http://www.biophysj.org/biophysj/supplemental/S0006-3495(17)31133-5.

AUTHOR CONTRIBUTIONS

F.B. and E.E.L.L. designed research, analyzed data, and wrote the manuscript. E.E.L.L. performed research. F.B. contributed analytic tools.

ACKNOWLEDGMENTS

We thank Li Tang for culturing rat dorsal root ganglion neurons and Dr. Michael Priest and Dr. Eduardo Perozo for editing. We give special thanks to Dr. João Carvalho-de-Souza for patch clamp training E.E.L.L.

REFERENCES

1. Baker, B. J., H. Mutoh, …, T. Knöpfel. 2008. Genetically encoded fluorescent sensors of membrane potential. *Brain Cell Biol.* 36:53–67.

2. Hochbaum, D. R., Y. Zhao, …, A. E. Cohen. 2014. All-optical electrophysiology in mammalian neurons using engineered microbial rhodopsins. *Nat. Methods.* 11:825–833.

3. Jin, L., Z. Han, …, V. A. Pieribone. 2012. Single action potentials and subthreshold electrical events imaged in neurons with a fluorescent protein voltage probe. *Neuron.* 75:779–785.

4. Lundby, A., W. Akemann, and T. Knöpfel. 2010. Biophysical characterization of the fluorescent protein voltage probe VSFP2.3 based on the voltage-sensing domain of Ci-VSP. *Eur. Biophys. J.* 39:1625–1635.

5. St-Pierre, F., J. D. Marshall, …, M. Z. Lin. 2014. High-fidelity optical reporting of neuronal electrical activity with an ultrafast fluorescent voltage sensor. *Nat. Neurosci.* 17:884–889.

6. Pédelacq, J.-D., S. Cabantous, …, G. S. Waldo. 2006. Engineering and characterization of a superfolder green fluorescent protein. *Nat. Biotechnol.* 24:79–88.

7. Yang, H. H., F. St-Pierre, …, T. R. Clandinin. 2016. Subcellular imaging of voltage and calcium signals reveals neural processing in vivo. *Cell.* 166:245–257.

8. Stefani, E., and F. Bezanilla. 1998. Cut-open oocyte voltage-clamp technique. *Enzymology.* 293:300–318.

9. Murata, Y., H. Iwasaki, …, Y. Okamura. 2005. Phosphoinositide phosphatase activity coupled to an intrinsic voltage sensor. *Nature.* 435:1239–1243.

10. Villalba-Galea, C. A., W. Sandtner, …, F. Bezanilla. 2009. Charge movement of a voltage-sensitive fluorescent protein. *Biophys. J.* 96:L19–L21.

11. Lacroix, J. J., and F. Bezanilla. 2012. Tuning the voltage-sensor motion with a single residue. *Biophys. J.* 103:L23–L25.

12. Carvalho-de-Souza, J. L., and F. Bezanilla. 2017. Voltage dependence and non-sensor residues. *Biophys. J.* 112:246a.

13. Li, Q., S. Wanderling, …, E. Perozo. 2014. Structural mechanism of voltage-dependent gating in an isolated voltage-sensing domain. *Nat. Struct. Mol. Biol.* 21:244–252.